



Cite this: *RSC Appl. Polym.*, 2026, **4**, 278

Tandem CO₂ valorisation to polycarbonate vitrimer and ethylene carbonate

Seiyoung Yoon, ^a Ling-Jo Wu, ^a Sophia Aracri, ^a Satej S. Joshi, ^a Vishal Kumar, ^b Wenbin Kuang, ^b Mark D. Foster, ^a James M. Eagan ^{*a} and Junpeng Wang ^{*a}

The need for renewably sourced polymers has intensified with the worsening of global challenges such as emissions and plastic pollution. Here, we report a CO₂-based poly(cyclohexene carbonate) (PCHC) vitrimer cured with zinc stearate that directly addresses both issues. Enhanced zinc dispersion within the network enabled faster curing and reprocessing than possible with zinc acetate systems, while maintaining consistent T_g and mechanical integrity across multiple cycles. The vitrimer undergoes rapid glycolysis in ethylene glycol, valorisation into ethylene carbonate with up to 97% yield without additional catalyst. When applied to carbon fibre-reinforced polymers (CFRPs), applying this strategy enabled the development of sustainable CO₂-based CFRP that can undergo full resin valorisation and recovery of clean, damage-free fibres. Collectively, this tandem CO₂ valorisation strategy—from vitrimer synthesis to fibre-reinforced composites and subsequent chemical valorisation—establishes multiple recycling and valorisation pathways and provides a promising route for carbon capture and utilization as well as material recycling.

Received 6th October 2025,
Accepted 17th November 2025

DOI: 10.1039/d5lp00314h

rsc.li/rscapplpolym

Introduction

Traditional polymer design strategies emphasized stability and performance, but the resulting durability has contributed to persistent global polymer waste. The persistence of conventional polymers in the environment and the difficulty of recycling them have intensified global concerns over plastic waste and resource preservation. Consequently, the need for sustainable alternatives to conventional polymers, particularly thermosetting polymers, has never been more urgent.

Owing to their easily tuneable mechanical properties through substrate and crosslink density manipulation, along with their high resistance to creep and stress relaxation, the use of thermosets has increased over the past few decades in fields such as construction,^{1,2} 3D printing,^{3,4} solid-state batteries,^{5–7} adhesives,^{2,8} and coatings.^{2,9} In particular, their great stiffness and fatigue resistance have made thermosets the dominant polymer used in the field of carbon fibre reinforced polymers (CFRPs).^{2,10–12} Due to their light weight, high strength, and excellent chemical resistance, thermoset composites are widely used in high-demand applications such as wind turbines, aircraft, and spacecraft.

However, in contrast to thermoplastics, thermosets typically cannot be repaired or healed once damaged due to their resistance to flow at elevated temperatures. In other words, thermosets cannot be subjected to mechanical recycling into the same application. Even minor damage in thermoset composites can lead to large cracks or delamination, necessitating complete replacement. Consequently, the increased use of thermosets further reinforces the already problematic linear economy of polymers.

Vitrimers,^{12–16} polymer networks whose strands or cross-links can undergo dynamic bond-exchange reactions (BERs) at elevated temperatures, are regarded by many researchers as potential alternatives to thermosets, since these reactions enable flow above the topology freezing temperatures (T_v), a temperature at which the stress relaxation and creep become noticeable. However, the presence of such BERs mean that vitrimers behave like thermoplastics at elevated temperatures, thereby compromising their thermal stability. Moreover, even at temperatures below T_v , vitrimers undergo slow BERs and exhibit long-term creep and stress relaxation at slow rates above their glass-transition temperature (T_g).^{17–21} Such dimensional instability is especially detrimental in CFRP fabrication as disorientation and delamination of fabrics can occur.

While multiple strategies have been explored to increase the thermal and dimensional stability of the vitrimer materials,^{19,22–24} BERs are easily suppressed under T_g .¹⁶ Therefore, increasing the T_g of the vitrimer substrate offers a straightforward means of enhancing both the thermal and

^aSchool of Polymer Science and Polymer Engineering, The University of Akron, Akron, Ohio 44325-3909, USA. E-mail: eagan@uakron.edu, jwang6@uakron.edu

^bEnergy and Environment Directorate, Pacific Northwest National Laboratory, Richland, Washington, USA



dimensional stability. Such improvements allow vitrimers to be substituted for thermosets in CFRP applications while providing enhanced reprocessability.

We have previously developed the CO_2 -based poly(cyclohexene carbonate) (PCHC) vitrimer system that valorises CO_2 into a high- T_g polycarbonate network.²⁵ The material exhibited excellent mechanical properties with no sign of creep for $T < T_g$. Although the material exhibited minimal creep up to 165 °C, successful reprocessing was demonstrated at 160 °C at high pressure (*ca.* 13.8 MPa compressive force). Furthermore, the material could be depolymerized into *trans*-cyclohexene carbonate and subsequently repolymerized back to vitrimer. Hence, CO_2 was valorised into a mechanically and chemically recyclable network with superior properties.

We envisioned that modifying the transesterification catalyst to improve dispersion and catalysis of BERs can further enhance the mechanical and chemical recyclability of the system. Such improvement would allow the vitrimer material to be more evenly incorporated into sustainable CFRP, where further chemical valorisation of the resin could enable fibre recovery. Herein, we demonstrate a tandem CO_2 valorisation strategy: first into recyclable and upcyclable polycarbonate vitrimer for lightweight, recyclable CFRP, and subsequently, glycolysis into ethylene carbonate at the end of service life, enabling recovery of carbon fibre from CFRP (Fig. 1).

Results and discussion

We prepared the same tri-functional acid-capped PCHC prepolymer from CO_2 , in a manner similar to that used with our previously-reported CO_2 -based PCHC vitrimer platform. This prepolymer served as the precursor for vitrimer network formation. In the network synthesis, carboxylic acids from malic acid and the acid-capped PCHC prepolymer reacted with the epoxide groups of DGEBA, generating β -hydroxy ester bonds that can undergo dynamic BERs (Fig. S1).²⁵

In our previous report, we surveyed three Lewis acid catalysts (antimony oxide, tin octoate, and zinc acetate), and zinc acetate was identified as the optimal curing catalyst, as it suc-

cessfully cured the network without decomposition. However, poor dispersion of zinc aggregates was observed, which can act as reinforcing fillers and suppressed macroscopic creep. Dispersion improved upon reprocessing. While the suppression of creep and the associated enhancement in mechanical performance are beneficial for the resin itself,²⁵ the presence of aggregates can introduce microdefects in CFRPs that could propagate along the fibre–matrix interface and eventually lead to interfacial debonding or delamination.^{11,26–28} To promote better dispersion of zinc in the PCHC vitrimer matrix, zinc stearate was selected due to its lower melting point and superior solubility in organic media.

The curing kinetics profiles of the PCHC vitrimer resin with zinc stearate suggest better dispersion of zinc ions into the network. While 5 mol% of zinc acetate was used to enable curing up to 100% gel fraction in the previous report,²⁵ the same equivalence of zinc stearate resulted in decomposition of the network at 150 °C (Fig. 2b and S2). Such decomposition is likely due to the higher incorporation of zinc ions into the network as all zinc catalysts are chemically dispersed into the network without agglomeration. Additionally, unlike acetic acid from zinc acetate, the stearic acid from zinc stearate remains in the network after curing and can further catalyse the transesterification and transcarbonation to induce backbiting decomposition of PCHC (Fig. S3).

Optimal curing of PCHC vitrimer was achieved upon reducing the equivalence of the zinc stearate. At 3 mol% of zinc stearate, the network reached a gel fraction above 90% upon 4 h of heating at 150 °C (Fig. 2b). It was also confirmed that post-curing for 4 h from 4 h to 8 h can slightly increase the gel fraction of the network without decomposition (Fig. 2b).

Non-isothermal creep experiments were conducted to characterize and compare the BERs of vitrimers with zinc stearate and zinc acetate catalysts. The sample containing 3 mol% zinc stearate exhibited slightly greater creep than the sample with 5 mol% zinc acetate (Fig. S4). This enhanced creep behaviour can be attributed to the combined catalytic activity of the zinc complex and residual stearic acid, which resulted in the 3 mol% zinc stearate system creeping more than the 5 mol% zinc acetate system despite its lower zinc content.

Manas-Zloczower *et al.* reported that density functional theory (DFT) calculations predicted zinc stearate to have an activation energy comparable to that of zinc acetate.²⁹ Interestingly, their experimental results did not follow the DFT predictions. Vitrimer materials with zinc stearate showed much slower stress relaxation, which they attributed to the large molar mass of zinc stearate acting as a filler, as well as counterion mobility and network inhomogeneities. In our system, inefficient dispersion of zinc acetate similarly caused zinc aggregates to act as fillers, suppressing creep despite the comparable activation energies predicted for zinc stearate and zinc acetate. In contrast, the efficient dispersion of zinc stearate promoted slightly greater creep than that observed for zinc acetate catalysed vitrimers.

The temperature sweep experiment revealed that the vitrimer with 3 mol% zinc stearate possessed a lower crosslinking

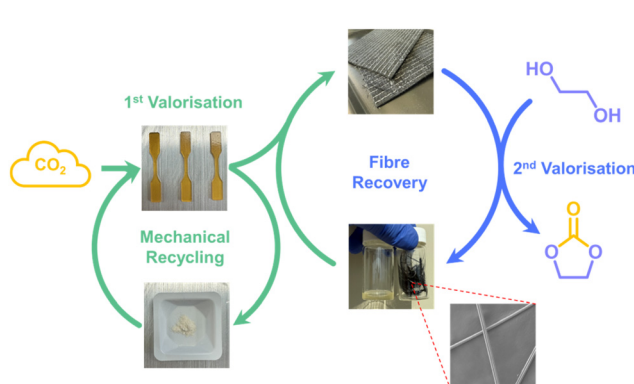


Fig. 1 Tandem valorisation of CO_2 into CO_2 -based vitrimer, composite and ethylene carbonate.



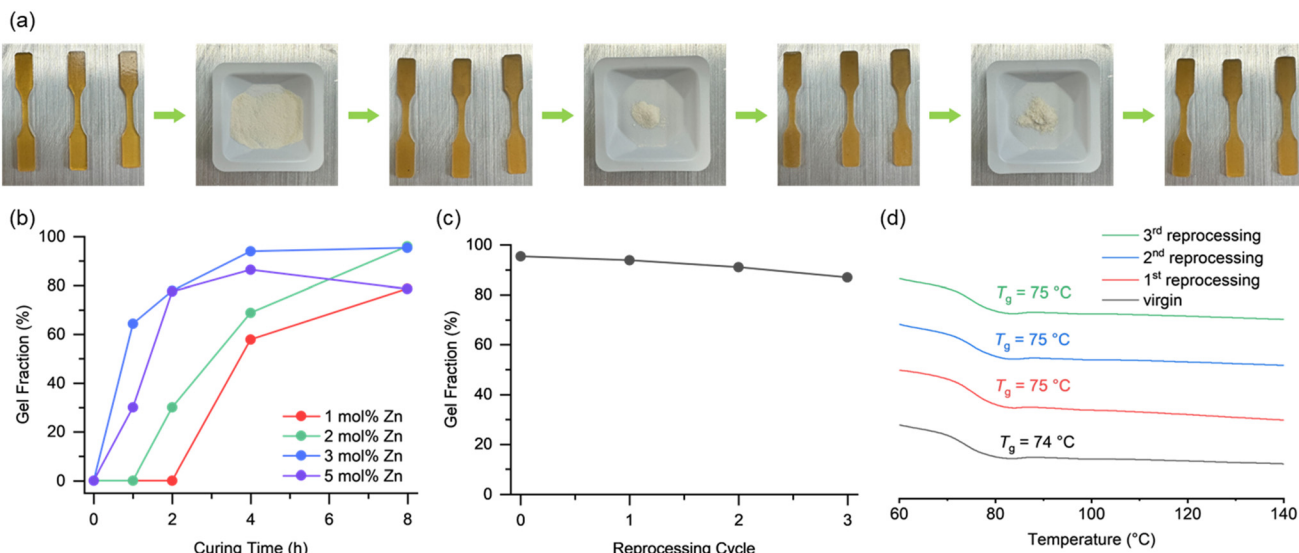


Fig. 2 Curing and reprocessing of poly(cyclohexene carbonate) (PCHC) vitrimer with zinc stearate. (a) Photos of PCHC samples in reprocessing cycles. (b) Curing kinetics of PCHC vitrimer with different amounts of zinc stearate catalyst at 150 °C. (c) Gel fraction of the sample with 3 mol% zinc stearate at each reprocessing cycle. (d) Differential scanning calorimetry (DSC) curves of the sample with 3 mol% zinc stearate at each reprocessing cycle with corresponding value of glass-transition temperature.

density than did the system with 5 mol% zinc acetate. This difference arises from the lower extent of zinc incorporation, as zinc ions additionally serve as crosslinking centres within the network (Fig. S5).

The increased catalytic activity of the PCHC vitrimer network with 3 mol% zinc stearate was also observed during the demonstration of mechanical recycling of the resin. To minimize mechanochemical degradation^{30–33} of the network and promote particle–particle contact of the ground resin,³⁴ the PCHC vitrimer samples were cryogenically ground *via* ball-milling at –196 °C for 10 min to produce a fine powder of PCHC vitrimer. Upon pressing at 160 °C for 2 h (Fig. 2a) the powder coalesced to high quality samples with minimal reduction in gel fraction. In contrast, the samples in the previous report with zinc acetate required 4 h of heated pressing. This highlights that the enhanced catalytic activity of zinc stearate accelerated the reprocessing of the PCHC vitrimer network.

The PCHC vitrimer resin was successfully reprocessed for up to three cycles with minimal reduction in gel fraction and no change in T_g (Fig. 2c and d). In contrast, vitrimer materials with zinc acetate previously showed an increase in T_g upon reprocessing due to improved catalyst dispersion.²⁵ The unchanging T_g of the PCHC vitrimer with zinc stearate implies that the extent of zinc incorporation was already at a maximum in the virgin samples. The combination of rapid reprocessing and stable zinc incorporation highlights the enhanced mechanical recyclability of the network, consistently maintained from the virgin samples to subsequent reprocessing cycles. Furthermore, the fast BERs that enable fast reprocessing also provide potential for facile chemical decomposition when desired.

Having established the mechanical recyclability of the vitrimer resin, we next evaluated its chemical deconstruction in resin and in CFRPs. While the synthesis of CO₂-based PCHC vitrimer itself represents a successful valorisation of CO₂, resolving the zinc dispersion issue and enhancing recyclability with zinc stearate further establishes this system as a promising platform for CO₂-based PCHC CFRP composites, thereby extending CO₂ valorisation from vitrimer resins to sustainable CFRPs.

Previously we had demonstrated chemical recycling through addition of extra catalyst to induce backbiting depolymerization of PCHC into *trans*-cyclohexene carbonate. However, this approach requires additional catalyst, elevated temperature, and vacuum. In addition, residual vitrimer components would remain on the fibres after depolymerization, meaning that the process achieves only partial recycling.

From an economic perspective, recovery of fibre is more important than the recycling of PCHC resin. One of the reasons the depolymerization of PCHC is challenging is the relatively high ring-strain energy of the *trans*-cyclohexene carbonate, which leads to a high ceiling temperature and necessitates high temperature for depolymerization. Therefore, we envisioned that using low-cost ethylene glycol to form ethylene carbonate with low ring-strain energy would accelerate the resin decomposition and promote fibre recovery.

To validate the approach, valorisation of the PCHC vitrimer resin into ethylene carbonate was conducted (Fig. 3). Since zinc stearate was already fully dispersed within the network, no additional catalyst was necessary. According to the curing kinetics reported previously,²⁵ the PCHC vitrimer with zinc acetate decomposed above 180 °C; therefore, vitrimer samples with zinc stearate were subjected to decomposition at 180 °C.



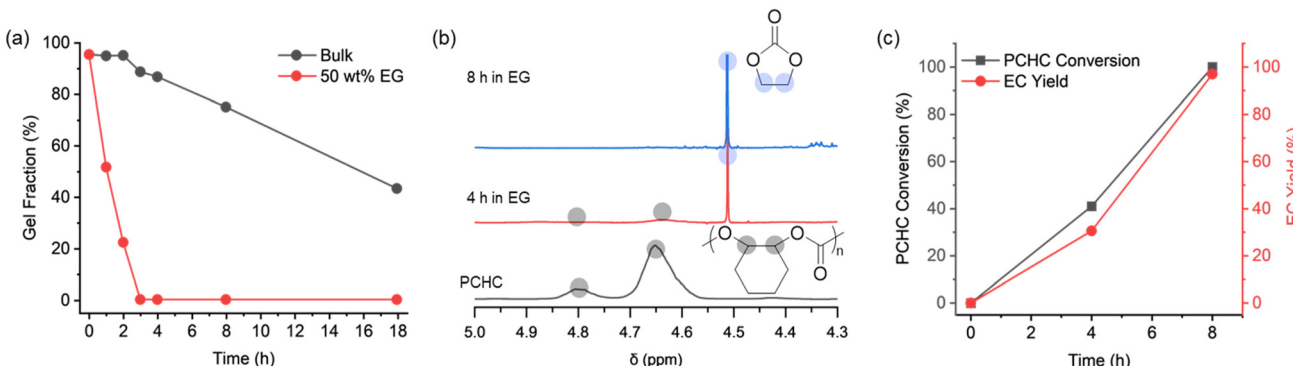


Fig. 3 Chemical valorisation of PCHC vitrimer resin. (a) Gel fraction as a function of treatment time in bulk and in 50 weight% ethylene glycol at 180 °C. (b) Nuclear magnetic resonance (NMR) spectroscopy of PCHC and aliquots after 4 h and 8 h of treatment in ethylene glycol. (c) Conversion of PCHC and yield of ethylene carbonate at different times of ethylene glycolysis.

When the vitrimer was heated without ethylene glycol, the gel fraction decreased to 43% after 18 h at 180 °C, indicating that simple heating of the PCHC vitrimer resin requires prolonged heating at high temperature and is therefore not ideal for decomposition strategy (Fig. 3a). The sol fraction was majorly composed with PCHC and DGEBA, suggesting that not much decrosslinking from *trans*-cyclohexene carbonate formation

occurred (Fig. S9). In contrast, heating the PCHC vitrimer samples in ethylene glycol (with a weight equal to that of the sample) significantly accelerated the decomposition, with the decomposition rate increasing with temperature. Notably, the PCHC vitrimer resin was completely decomposed (0% gel fraction) upon 3 h of heating at 180 °C (Fig. 3a). For comparison, glycolysis was performed on PCHC vitrimers with zinc acetate

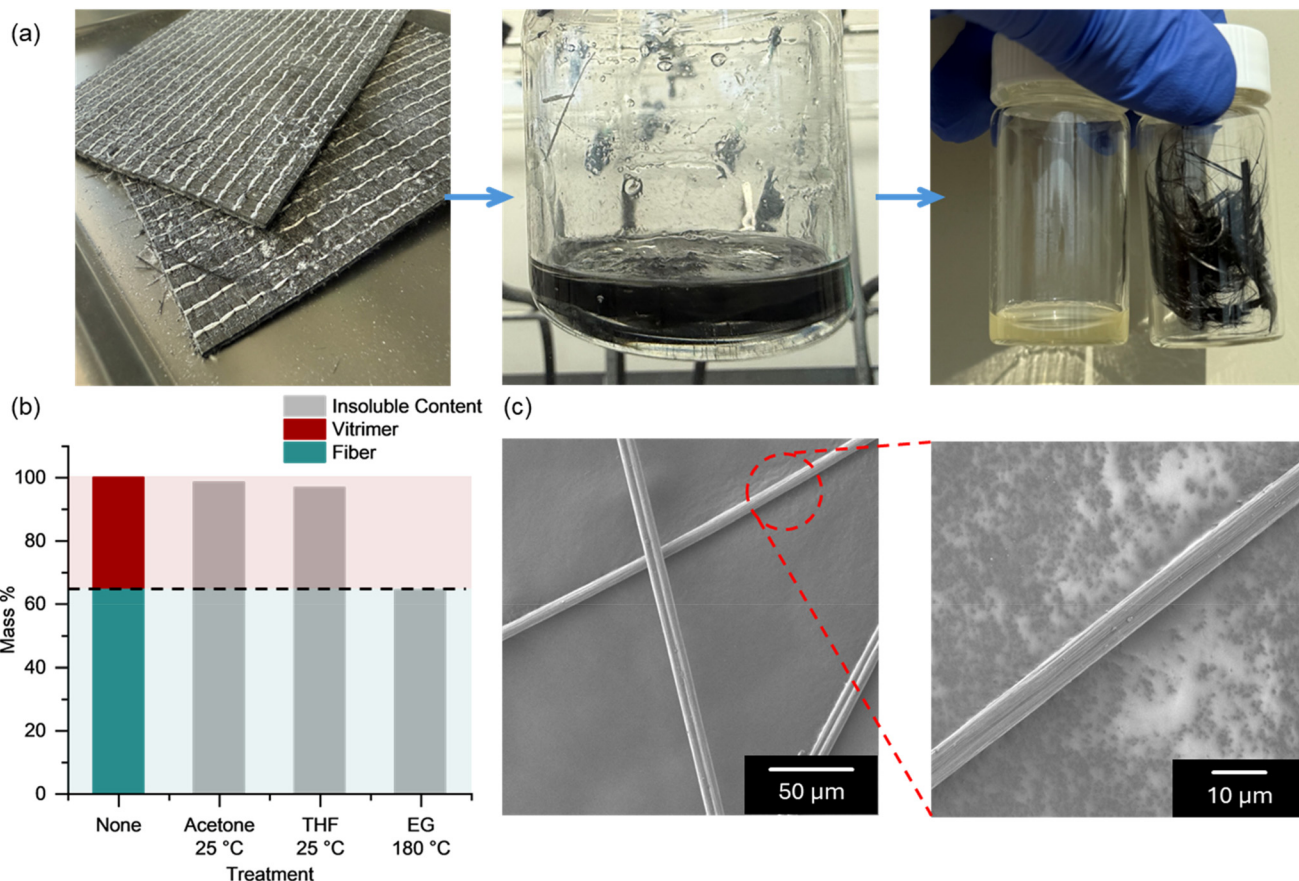


Fig. 4 Chemical valorisation of carbon fibre-reinforced vitrimer composite. (a) Photos of composite undergoing ethylene glycolysis to be separated into valorised resin and fibres. (b) Mass % of the insoluble content after solvolysis treatments. (c) SEM images of recovered fibres.

and on thermosets without external catalysts. The role of catalytic activity was evident—while the catalyst-free thermoset retained 20% gel fraction after 16 h, the vitrimer containing zinc acetate achieved complete resin digestion (0% gel fraction) within 8 h. The low catalytic activity of the vitrimer containing zinc acetate can be attributed to the reduced incorporation of zinc ions caused by catalyst agglomeration, as evidenced by the slower curing kinetics.

Nuclear magnetic resonance (NMR) spectroscopy of the decomposed mixture from zinc stearate catalysed vitrimer suggests 39% conversion of the PCHC backbone and 30% yield of ethylene carbonate after 4 h of heating at 180 °C (Fig. 3b, c and S6). Upon further heating for 4 h (8 h in total), full conversion of PCHC backbone was achieved with 96% yield of ethylene carbonate (according to BHT signals as internal standards) (Fig. 3b, c and S7). Upon vacuum distillation, 73% yield of spectroscopically pure ethylene carbonate was separated (Fig. S10). The high yield of ethylene carbonate highlights the efficient valorisation mechanism with minimal side reactions.

PCHC CFRP was prepared *via* hand layup process and heat pressing at 150 °C. Before applying this valorisation strategy to the CFRPs, the chemical stability of the PCHC CFRP was assessed. PCHC CFRP samples containing 65 wt% fibre were immersed in acetone and THF. Almost no mass loss or fibre disorientation was observed, confirming full curing and effective binding of the PCHC resin to the fibres (Fig. 4b and S9).

In contrast, when the PCHC CFRP was immersed in ethylene glycol for resin digestion, the fibres began to disorient and detach from the matrix after heating at 180 °C for 3 h. After washing with THF, the remaining insoluble content was 71%, indicating that although some resin remained between the fibres, most of the matrix had been digested. After prolonged heating at 180 °C for 16 h, fibres were successfully separated from the resin. Upon separation, the fibres were washed with THF to remove residual resin (Fig. 4a). The remaining insoluble content after drying was 64.3 wt%, suggesting that all the resin was separated from the fibres (Fig. 4b). The ¹H NMR spectrum of the separated resin further suggests full conversion of PCHC backbone into ethylene carbonate, which facilitated the resin and fibre separation (Fig. S8). The SEM images of the recovered fibres showed fibres with almost no leftover resin on their surfaces (Fig. 4c and S10). Together, these results demonstrate effective valorisation of the PCHC vitrimer resin into ethylene carbonate and recovery of clean fibres, highlighting a successful tandem CO₂ valorisation from vitrimer to CFRP and ultimately to ethylene carbonate.

Conclusions

To conclude, we developed a CO₂-based PCHC vitrimer that can be efficiently cured with zinc stearate to yield a high-*T_g* resin with excellent mechanical reprocessability. Improved zinc dispersion in the vitrimer network enabled faster curing

and reprocessing compared to previous systems, while maintaining consistent *T_g* and mechanical integrity across multiple cycles of reprocessing, making the CO₂-based PCHC vitrimer a suitable platform for CFRPs. The PCHC vitrimer resin undergoes fast and complete glycolysis into ethylene carbonate, enabling further chemical valorisation of the incorporated CO₂ in high yield. When implemented into CFRPs, this strategy enables efficient resin degradation and clean fibre recovery, thereby demonstrating both the chemical valorisation of the PCHC vitrimer and the effective recovery of carbon fibres. These results establish multi-step valorisation of CO₂. We envision that this tandem CO₂ valorisation strategy will inspire future designs of carbon fibre-reinforced thermoset composites and provide a promising route toward carbon neutrality and polymer sustainability by transforming CO₂ into recyclable and upcyclable materials.

Author contributions

Conceptualization – SY, JME, JW. Funding acquisition – WK, MDF, JME, JW. Methodology – SY. Resources – SY, SSJ, VK. Supervision – WK, MDF, JME, JW. Validation – SY, LJW, SA. Writing – original draft – SY. Writing – review & editing – SY, LJW, SA, SSJ, VK, WK, MDF, JME, JW.

Conflicts of interest

The authors declare the following competing financial interest (s): SSJ, SY, SA, MDF, JW, JME are inventors on a patent application of the subject materials and JME owns equity in Eterno LLC., commercializing CO₂-based thermosets.

Data availability

The data supporting this article have been included as part of the supplementary information (SI). Supplementary information: detailed experimental procedures and characterization data NMR, SEM, non-isothermal creep, temperature sweep, curing kinetics. See DOI: <https://doi.org/10.1039/d5lp00314h>.

Acknowledgements

This material is based upon work supported by the U.S. Department of Energy's Office of Energy Efficiency and Renewable Energy (EERE) under the Advanced Materials and Manufacturing Technologies Office (AMMTO) Award Number DE-EE0009297. J. W. acknowledges the Camille and Henry Dreyfus Foundation for a Camille Dreyfus Teacher-Scholar Award (TC-24-087).

References

1 S. Agarwal and R. K. Gupta, in *Thermosets (Second Edition)*, ed. Q. Guo, Elsevier, 2018, pp. 279–302, DOI: [10.1016/B978-0-08-101021-1.00008-3](https://doi.org/10.1016/B978-0-08-101021-1.00008-3).

2 D. Ratna, in *Recent Advances and Applications of Thermoset Resins (Second Edition)*, ed. D. Ratna, Elsevier, 2022, pp. 1–172, DOI: [10.1016/B978-0-323-85664-5.00006-5](https://doi.org/10.1016/B978-0-323-85664-5.00006-5).

3 I. D. Robertson, M. Yourdkhani, P. J. Centellas, J. E. Aw, D. G. Ivanoff, E. Goli, E. M. Lloyd, L. M. Dean, N. R. Sottos, P. H. Geubelle, J. S. Moore and S. R. White, *Nature*, 2018, **557**, 223–227.

4 X. Kuang, Z. Zhao, K. Chen, D. Fang, G. Kang and H. J. Qi, *Macromol. Rapid Commun.*, 2018, **39**, 1700809.

5 F. Baskoro, H. Q. Wong and H.-J. Yen, *ACS Appl. Energy Mater.*, 2019, **2**, 3937–3971.

6 B. S. Lalia, T. Fujita, N. Yoshimoto, M. Egashira and M. Morita, *J. Power Sources*, 2009, **186**, 211–215.

7 C. Wu and W. Zeng, *Chem. – Asian J.*, 2022, **17**, e202200816.

8 T. Engels, in *Thermosets (Second Edition)*, ed. Q. Guo, Elsevier, 2018, pp. 341–368, DOI: [10.1016/B978-0-08-101021-1.00010-1](https://doi.org/10.1016/B978-0-08-101021-1.00010-1).

9 F. Aguirre-Vargas, in *Thermosets (Second Edition)*, ed. Q. Guo, Elsevier, 2018, pp. 369–400, DOI: [10.1016/B978-0-08-101021-1.00011-3](https://doi.org/10.1016/B978-0-08-101021-1.00011-3).

10 M. Natali, J. M. Kenny and L. Torre, in *Thermosets (Second Edition)*, ed. Q. Guo, Elsevier, 2018, pp. 477–509, DOI: [10.1016/B978-0-08-101021-1.00015-0](https://doi.org/10.1016/B978-0-08-101021-1.00015-0).

11 M. Perner, S. Algermissen, R. Keimer and H. P. Monner, *Robot. Comput.-Integr. Manuf.*, 2016, **38**, 82–92.

12 V. Kumar, W. Kuang and L. S. Fifield, *Materials*, 2024, **17**, 3265.

13 M. Capelot, M. M. Unterlass, F. Tournilhac and L. Leibler, *ACS Macro Lett.*, 2012, **1**, 789–792.

14 D. Montarnal, M. Capelot, F. Tournilhac and L. Leibler, *Science*, 2011, **334**, 965–968.

15 M. Röttger, T. Domenech, R. van der Weegen, A. Breuillac, R. Nicolaï and L. Leibler, *Science*, 2017, **356**, 62–65.

16 W. Denissen, J. M. Winne and F. E. Du Prez, *Chem. Sci.*, 2016, **7**, 30–38.

17 A. M. Hubbard, Y. Ren, D. Konkolewicz, A. Sarvestani, C. R. Picu, G. S. Kedziora, A. Roy, V. Varshney and D. Nepal, *ACS Appl. Polym. Mater.*, 2021, **3**, 1756–1766.

18 L. Li, X. Chen, K. Jin and J. M. Torkelson, *Macromolecules*, 2018, **51**, 5537–5546.

19 F. Van Lijsebetten, K. De Bruycker, Y. Spiesschaert, J. M. Winne and F. E. Du Prez, *Angew. Chem., Int. Ed.*, 2022, **61**, e202113872.

20 F. Van Lijsebetten, T. Debsharma, J. M. Winne and F. E. Du Prez, *Angew. Chem., Int. Ed.*, 2022, **61**, e202210405.

21 G. Singh, V. Varshney and V. Sundararaghavan, *Polymer*, 2024, **313**, 127667.

22 R. G. Ricarte, F. Tournilhac, M. Cloître and L. Leibler, *Macromolecules*, 2020, **53**, 1852–1866.

23 R. G. Ricarte, F. Tournilhac and L. Leibler, *Macromolecules*, 2019, **52**, 432–443.

24 J. P. Brutman, D. J. Fortman, G. X. De Hoe, W. R. Dichtel and M. A. Hillmyer, *J. Phys. Chem. B*, 2019, **123**, 1432–1441.

25 S. Yoon, S. S. Joshi, S. Aracri, Y. Ospina-Yepes, D. Sathe, M. D. Foster, J. Wang and J. M. Eagan, *ACS Appl. Polym. Mater.*, 2025, **7**, 4561–4571.

26 Y. Li, B. Wang and L. Zhou, *Eng. Failure Anal.*, 2023, **153**, 107576.

27 Y. S. Petronyuk, V. M. Levin, E. S. Morokov, T. B. Ryzhova, A. V. Chernov and I. V. Gulevsky, *Bull. Russ. Acad. Sci.: Phys.*, 2016, **80**, 1224–1228.

28 C. Xie, Z. Zhao, L. Sun, J. Wang, J. Jiang and Y. Li, *Compos. Struct.*, 2025, **354**, 118828.

29 A. Jamei Oskouei, E. Mao, T. G. Gray, A. Bandegi, S. Mitchell, M. K. Sing, J. Kennedy, K. M. McLoughlin and I. Manas-Zloczower, *RSC Appl. Polym.*, 2024, **2**, 905–913.

30 S. Cha, J. G. Kim and G. I. Peterson, *Macromolecules*, 2024, **57**, 9960–9964.

31 E. Jung, D. Yim, H. Kim, G. I. Peterson and T.-L. Choi, *J. Polym. Sci.*, 2023, **61**, 553–560.

32 J. Noh, G. I. Peterson and T.-L. Choi, *Angew. Chem., Int. Ed.*, 2021, **60**, 18651–18659.

33 G. I. Peterson, W. Ko, Y.-J. Hwang and T.-L. Choi, *Macromolecules*, 2020, **53**, 7795–7802.

34 H. Li, B. Zhang, K. Yu, C. Yuan, C. Zhou, M. L. Dunn, H. J. Qi, Q. Shi, Q.-H. Wei, J. Liu and Q. Ge, *Soft Matter*, 2020, **16**, 1668–1677.

